Published in final edited form as:

Matrix Biol. 2020 July ; 89: 43–58. doi:10.1016/j.matbio.2020.01.001.

PGC1α suppresses kidney cancer progression by inhibiting collagen-induced SNAIL expression

Hyeyoung Nam[1], **Anirban Kundu**[1], **Garrett J. Brinkley**[1], **Darshan S. Chandrashekar**[2], **Richard L. Kirkman**[1], **Balabhadrapatruni V. S. K. Chakravarthi**[2], **Rachael M. Orlandella**[3], **Lyse A. Norian**[4], **Guru Sonpavde**[5], **Pooja Ghatalia**[6], **Fei Fei**[2], **Shi Wei**[2], **Sooryanarayana Varambally**[2], **Sunil Sudarshan**[1]

[1]Department of Urology, University of Alabama at Birmingham, Birmingham, AL, 35294

[2]Department of Pathology, University of Alabama at Birmingham, Birmingham, AL, 35294

[3]Graduate Biomedical Science, Nutrition Obesity Research Center, University of Alabama at Birmingham, Birmingham, AL, 35294

[4]Department of Nutrition Sciences, Comprehensive Cancer Center, Nutrition Obesity Research Center, University of Alabama at Birmingham, AL, 35294.

[5]Department of Medical Oncology, Dana Farber Cancer Institute, MA, 02215

[6]Department of Hematology/Oncology, Fox Chase Cancer Center, Philadelphia, PA, 19111

Abstract

The transcriptional events that promote invasive and metastatic phenotypes in renal cell carcinoma (RCC) remain poorly understood. Here we report that the decreased expression of peroxisome proliferator-activated receptor gamma, coactivator 1 alpha (PGC1α) and the increased expression of several genes encoding collagen family members are associated with RCC tumor progression. PGC1α restoration attenuates invasive phenotypes and suppresses tumor progression *in vivo*. In contrast, collagens produced by RCC cells promote invasive and migratory phenotypes. PGC1α restoration suppresses the expression of collagens and tumor phenotypes via the induction of *miR-29a*. Furthermore, decreased collagens via the PGC1α*/miR-29a* axis suppresses collagen-mediated activation of discoidin domain receptor 1 (DDR1)/ERK signaling. In turn, the suppression of collagen/DDR1 signaling by PGC1α leads to decreased levels of the known EMT

Address correspondence to: Sunil Sudarshan, Department of Urology, University of Alabama at Birmingham, Birmingham, AL, 1105 Faculty Office Tower, 510 20th Street South, Birmingham, AL 35294, USA. Phone: 205-996-8765; Fax: 205-934-4933; ssudarshan@uabmc.edu.

Author contributions

H. N. and S.S. designed the research and analyzed the experiments and wrote the manuscript. D.S.C. and S.V. generated and analyzed the bioinformatics data. A.K., G.J.B. and R.L.K. performed *in vitro* experiments. B.V.S.K.C., R.M.O, L.A.N, F.F., and S.W. helped with the *in vivo* experiments. G.S. and P.G. collected the human samples.

Declaration of Interests

The authors declare no competing interests.

We certify that there is no conflict of interest with any financial organization regarding the material described in this manuscript.

regulators SNAIL1 and *2*. Collectively, our results demonstrate a novel role for PGC1α in the regulation of proinvasive SNAIL proteins.

Introduction

Kidney cancer accounts for over 14,000 deaths in the United States annually [1]. The most common subtype of renal cancer (~75%) is clear cell renal cell carcinoma (ccRCC) [2]. Inactivation of the *VHL* gene is a common initiating event in primary ccRCC which results in stabilization of hypoxia inducible factors (HIFs) and subsequent upregulation of hypoxia-responsive genes. Several current therapeutic approaches to RCC are based on the VHL/HIF pathway. Tumor progression to metastasis is the major cause of the mortality associated with RCC. Patients with metastasis have a median survival of 2~3 years despite several available therapies, including immunotherapy and antiangiogenic agents. In contrast, patients with tumors confined to the kidney, including those with relatively large tumors, have far more favorable outcomes with appropriate treatment. Large scale data sets such as The Cancer Genome Atlas (TCGA) research network have been integral to our understanding of RCC biology. However, these data sets have focused on primary tumors. In contrast, data examining metastatic tissues from RCC patients are lacking, thereby limiting the current knowledge of the molecular underpinnings of disease progression.

PPARGC1A encodes for the transcription factor peroxisome proliferator activated receptor γ coactivator 1α (PGC1α). PGC1α is highly expressed in tissues with high energy demands and abundant mitochondria, including brown adipose and kidney tissues [3, 4]. PGC1α interacts with several other transcription factors that facilitate an increased capacity for cellular energy production, mitochondrial biogenesis, and fatty acid oxidation [5, 6]. Although emerging evidence indicates that PGC1α plays a crucial role in cancer metabolism, PGC1α has been shown to have both pro- and anti-tumorigenic effects. These findings suggest that the role of PGC1α in cancer is likely to be context and tissue dependent. To date, mechanistic studies on PGC1α's role in invasive ccRCC phenotypes have not been reported.

Abnormalities of the extracellular matrix (ECM), a complex and dynamic network of macromolecules, may also affect tumor migration and metastasis [7]. The major components of the ECM are fibrous proteins such as collagens, which account for about 30% of proteins in the human body [8, 9]. Excess accumulation of collagen family members is well described in chronic kidney disease and is the hallmark of kidney fibrosis[10]. Studies on collagen in cancer have primarily focused on collagen synthesized by cancer-associated fibroblasts; however, less is known about collagen production by tumor cells. *COL23A1*, a collagen family member, was recently found to be highly expressed in ccRCC [11]. However, detailed mechanistic insight into the link between collagen and tumor progression in ccRCC is lacking.

Here, we demonstrate that PGC1α loss is a common feature of metastatic ccRCC. PGC1α restoration reduces migratory and invasive behaviors and suppresses metastasis in two independent *in vivo* models. PGC1α expression decreases SNAIL1/2 expression via reduced protein stability. In tandem, increased expression of several collagen genes is observed in

aggressive ccRCC. Collagens produced by RCC cells promote invasive and migratory phenotypes. In metastatic tumors, PGC1α expression is inversely correlated with the expression of collagen family members. Correspondingly, PGC1α restoration suppresses the gene expression of collagen family members via the induction of *miR-29a*. The suppression of collagen expression via the PGC1α*/miR-29a* axis leads to the inactivation of DDR1 (discoidin domain receptor) signaling. DDR1 is a transmembrane tyrosine kinase receptor known to bind with collagen [12, 13]. DDR1 inactivation eventually leads to the degradation of SNAIL1/2 protein. Taken together, these data indicate that PGC1α destabilizes SNAIL1/2 proteins via suppression of the collagen/DDR1 axis. Furthermore, these data indicate that modulation of PGC1α, or its downstream mediators, may have therapeutic potential for metastatic renal cancer.

Results

Transcriptomic analysis of RCC tumor progression

Normal kidney, primary, and metastatic ccRCC tumor deposits were analyzed by transcriptomic array analysis as recently reported (fig. S1A) [14]. We identified 22 differentially expressed probes associated with metastasis (table S1). One of the down-regulated probes was *PPARGC1A* which encodes for PGC1α (Fig. 1A). We further validated these data in a separate cohort of patient-matched samples. The decreased mRNA expression of *PGC1α* was found in both primary and metastatic tumor relative to patient-matched normal kidney (Fig. 1B). The protein levels of PGC1α were lower in RCC tumor tissues relative to uninvolved adjacent kidney (Fig. 1C). RCC cell lines also demonstrated lower expression of *PGC1α* mRNA relative to normal kidney tissue (Fig. 1D). Using data from TCGA data set, reduced *PGC1α* expression was associated with higher tumor grade in RCC (fig. S1B). In addition to PGC1α loss, we observed the increased expression of several genes encoding collagen family members (*COLs*) in metastasis (table S1). Although no significant induction of *COLs* was found in primary tumors, a significant upregulation of *COLs* was identified in metastatic tumor deposits relative to normal kidney and primary tumor based on microarray data (Fig. 1A). We next validated these data as well as examined the expression of other *COL* members in a separate cohort of patient-matched samples. Similar to our array data, the mRNA expression of *COLs* was predominantly increased in metastatic tissue as opposed to normal kidney and primary tumor (Fig. 1E). The increased expression of these *COLs*, including *COL1A1, COL5A1, COL6A2*, and *COL11A1* was associated with worse prognosis in the TCGA cohort (fig. S1C). In addition, the increased expression of multiple *COLs* was associated with higher tumor grade in RCC patients (fig. S1D–G). Increased transcript levels of *COLs* in metastatic samples from RCC patients could be from the tumor cells or other cells within the microenvironment[15]. We therefore characterized a panel of RCC cell lines for transcript levels of *COLs*. Notably, multiple RCC cell lines including CAKI-1, RXF-393, and OSRC2 displayed a higher expression of *COLs* transcripts compared to normal kidney (Fig. 1F). Consistent with the mRNA expression findings, COL1A1 protein levels were highly expressed in CAKI-1 and RXF-393 cells (Fig. 1G). The protein levels of COL6A2 were also detectable in CAKI-1, RXF-393, and OSRC-2 cells.

PGC1α suppresses collagen expression in a *miR-29a* dependent manner

We noted that RCC cell lines with lower mRNA expression of *PGC1α* (CAKI-1, RXF-393, and OSRC-2) tended to have higher *COL* expression (compare Fig. 1D with Fig. 1F–G). Further analysis of gene expression array data focused on metastatic tissues demonstrated an inverse relationship between *PGC1α* mRNA expression and the expression of several *COL* genes (fig. S2A). Given these findings, we assessed the effects of PGC1α restoration on *COL* expression in high *COL* expressing cell lines (CAKI-1 and RXF-393). Reconstitution of PGC1α in both CAKI-1 and RXF-393 cells reduced mRNA expression of *COLs* (Fig.2A and fig. S2B). Stable expression of PGC1α resulted in decreased protein levels of COL1A1, COL6A2, and COL11A1 in both CAKI-1 and RXF-393 cells (Fig. 2B). We initially considered if this finding could be mediated by TGF-β signaling, a known regulator of collagen transcription. However, no changes in phosphorylation of SMAD2 or SMAD3, downstream readouts of TGF-β signaling, were found in PGC1α expressing RCC cells (fig. S2C). Furthermore, chromatin immunoprecipitation (ChIP) analysis demonstrated no significant effect of PGC1α on SMAD3 binding to SMAD binding element (SBE) motifs in the promoter of the *COL1A1* gene (fig. S2D). PGC1α often cooperates with members of a family of nuclear receptors known as the estrogen-related receptors (*ERRs*) to exert its transcriptional effects [16]. We recently reported that the expression of *ESRRG* (encoding ERRγ) was reduced in RCC tumors [14]. We assessed the effect of ERRγ on the mRNA expression of *COLs* in CAKI-1 and RXF 393 cells. ERRγ expression did not reduce the expression of *COLs* in RCC cells (fig. S2E–F). Moreover, no additional effect on *COL* expression was observed when ERRγ was co-expressed with PGC1α (fig. S2E).

MicroRNAs (miRNAs) are a family of small non-coding RNA molecules that have been implicated in the regulation of *COL* genes [17, 18]. We thus performed miRNA profiling in RCC cells expressing an empty vector or PGC1α. In both CAKI-1 and RXF-393 cells, PGC1α induced the expression of *miR-29a* (Fig. 2C and fig. S3A). The increased expression of *miR-29a* via PGC1α was validated via qRT-PCR in both cell lines whereas PGC1α re-expression failed to induce the expression of *miR-29b* and *miR-29c* (Fig. 2D and fig. S3B). Prior studies indicate that all members of the *miR-29* family are down-regulated in primary RCC tumors relative to normal kidney [19]. However, studies on the expression and role of *miR-29a* in RCC metastasis are lacking. We observed that *miR-29a* expression is lower in metastatic tumor deposits relative to patient-matched normal kidney (Fig. 2E). Although metastatic samples trended toward lower *miR-29a* levels relative to primary tumors, these data did not reach statistical significance. CAKI-1 cells (high basal *COL* expression) transfected with *miR-29a* mimic led to lower *COL* mRNA levels (Fig. 2F). Correspondingly, RCC4 cells (low basal *COL* expression) transfected with a *miR-29a* antagomir led to increased mRNA expression of *COLs* (Fig. 2G). Moreover, treatment of PGC1α expressing RCC cells with *miR-29a* antagomir restored COL expression (Fig. 2H). Taken together, these findings indicate that the suppression of *COLs* by PGC1α is mediated via induction of *miR-29a*.

PGC1α suppresses invasive behavior and tumor progression in RCC

COL expression has been associated with aggressive behavior in other tumor types. Given our findings that PGC1α suppresses *COL* expression in RCC cells, we consider the

biological significance of PGC1α loss in ccRCC. We evaluated the role of PGC1α in tumor cell migration using a monolayer scratch healing assay. Ectopic PGC1α expression markedly attenuated wound closure compared to control cells in RCC cell lines (Fig. 3A–B). Similarly, PGC1α expression significantly reduced cell migration in RXF-393 cells via Boyden chamber assay (fig. S4A–B). In addition, PGC1α markedly suppressed the invasive phenotypes of CAKI-1 and RXF-393 cells as determined by an invasion chamber assay with Matrigel insert (Fig. 3C and fig. S4C). Given that enforced PGC1α suppressed migratory and invasive phenotype in RCC cells, we evaluated the effect of PGC1α on the metastasis of RCC cells using the *in vivo* chick embryo chorioallantoic membrane (CAM) assay as illustrated in fig. S4D. The CAM assay allows for the assessment of metastasis of human tumor cells to tissues in a quantitative manner by measuring human-specific Alu repeats in genomic DNA from extracted tissues. RXF-393 cells expressing either an empty vector or PGC1α were inoculated on the upper CAM of 10-day old chick embryos and incubated for 7 days. Ectopic PGC1α expression markedly attenuated the ability of RCC cells to metastasize to both lung and liver (Fig. 3D–E). Furthermore, we evaluated the role of PGC1α with an orthotopic model of RCC using SN12PM6-1 cells. SN12PM6-1 cells are luciferase expressing cells and capable of primary tumor growth as well as metastasis [20]. SN12PM6-1 cells transduced with an empty vector or PGC1α were injected into the left kidney of SCID mice (5 weeks old). Orthotopic injection of SN12PM6-1 control cells resulted in aggressive tumor burden (Fig. 3F and fig S4E–F). In addition, orthotopic injection of SN12PM6-1 control cells developed histologically detectable metastases in multiple organs including spleen and lung (Fig. 3G–I). In contrast, mice injected with SN12PM6-1 cells expressing PGC1α showed attenuated tumor burden at 6 weeks from tumor challenge. We confirmed the expression of PGC1α by analyzing the mRNA expression of TCA cycle enzymes, downstream targets of PGC1α, in orthotopic kidney tumors (fig. S4G). Furthermore, orthotopic tumors expressing PGC1α demonstrated reduced *COL* mRNA and protein expression consistent with our *in vitro* studies (Fig, 3J–K). Collectively, these data demonstrate that PGC1α suppresses RCC tumor progression and reduces COL expression *in vivo*.

PGC1α restoration inhibits SNAIL stabilization in RCC

Our data demonstrating that PGC1α suppresses metastatic phenotypes *in vivo* led us to examine the expression of markers related to EMT, a process known to increase the motility and invasiveness of tumor cells [21]. The expression of EMT markers including N-cadherin, Vimentin, TCF/ZEB1, β-catenin, SNAIL1/2, and TWIST1 were characterized in RCC cells expressing an empty vector or PGC1α. Of these, both SNAIL1 and 2 protein were decreased by PGC1α expression (Fig. 4A) whereas the expression of other EMT markers were not altered by PGC1α (fig. S4H). Consistently, analysis of a panel of RCC cell lines demonstrate that cells with detectable PGC1α expression (RCC4, 769-P, and CAKI-2) tended to have lower SNAIL1/2 levels compared with RCC cell lines without detectable PGC1α (Fig. 4B). PGC1α mediated reduction in SNAIL1/2 protein was not associated with a consistent effect on transcript levels (Fig. 4C). Furthermore, we examined the expression of SNAIL1/2 level in orthotopic kidney tumors. Consistent with our *in vitro studies,* PGC1α expressing orthotopic tumors demonstrated reduced SNAIL1/2 protein levels without effects on mRNA expression (Fig. 4D–E). Based on these data, we next performed loss of function

studies via siRNA mediated knockdown of PGC1α in RCC4 cells which have detectable PGC1α expression. We first confirmed knockdown with the siRNA construct (Fig. 4F). PGC1α knockdown resulted in increased levels of both SNAIL1 and SNAIL2 proteins compared to control siRNA (Fig. 4G). We next considered posttranscriptional effects as prior studies indicate that SNAIL protein is a highly unstable protein and degraded by the ubiquitin-proteasome system [22]. Decreased SNAIL1 protein levels in PGC1α expressing cells was rescued by incubation with proteasomal inhibitor MG132 (Fig. 4H). We therefore evaluated the effect of PGC1α on SNAIL protein stability. The kinetics of SNAIL1 protein stability were measured after blocking protein synthesis using the translation inhibitor cycloheximde (CHX). SNAIL1 protein was detectable at 2 hours in control cells with slower degradation (Fig. 4I–J). In contrast, SNAIL1 protein was almost completely degraded after 40 minutes in PGC1α expressing RCC cells. Collectively, these data indicate that PGC1α destabilizes SNAIL1 protein levels in RCC.

COL1A1 knockdown reduces SNAIL expression and tumor growth in RCC

We next investigated the biological significance of endogenous *COL* production by RCC cells. CAKI-1 cells (high basal *COL* expression) were allowed to invade the Matrigel gel pore membrane using a Boyden invasion chamber with fetal bovine serum (FBS) as the chemoattractant as illustrated in Fig. 5A. The non-invasive cells from inside the chamber as well as invasive cells from the bottom of the membrane were separately isolated and the expression of *COLs* was assessed. The mRNA expression of *COLs* was significantly increased in invasive cells compared to non-invasive cells (Fig. 5B). RNA-seq analysis of TCGA data on RCC demonstrates that the transcript levels of *COL1A1* and *COL6A2* are higher relative to other C*OLs* (Fig. 5C). *COL1A1* was ectopically expressed in RCC4 cells which have low basal *COL* expression (Fig. 5D). COL1A1 expression upregulated SNAIL1/2 protein levels in RCC4 cells (Fig. 5D). Correspondingly, CAKI-1 (high basal *COL* expression) stably transduced with two independent shRNA constructs to *COL1A1* had reduced SNAIL1/2 (Fig. 5E). Moreover, the migratory and invasive phenotypes were attenuated in *COL1A1* knockdown cells (Fig. 5F–H). As we previously demonstrated that PGC1α induces *miR-29a* and that *miR-29a* can suppress *COL1A1* expression (Fig. 2C, D, and F), we assessed the effects of *miR-29a* inhibition on PGC1α-expressing RCC cells. Notably, antagomiR-*29a* increased both SNAIL expression (Fig. 5I) and migratory phenotypes in RCC cells (Fig. 5J–K). Given these *in vitro* data, we assessed the functional significance of *COL1A1 in vivo.* Notably, *COL1A1* knockdown resulted in a significantly reduced growth of CAKI-1 xenografts (Fig. 5L–M).

PGC1α leads to a decrease in SNAIL protein expression via inhibition of the collagen-mediated DDR1 axis

We next considered the mechanism by which *COLs* promoted the observed phenotypes in RCC. Collagens are a major component of the extracellular matrix and are known to initiate signaling cascades through interaction with cell surface receptors, including integrins and receptor tyrosine kinases [23–25]. We noted that COL1A1 protein was readily detectable in the conditioned media (CM) of CAKI-1 and RXF-393 cells which have high basal *COL* expression (Fig. 6A, lanes 1 and 3). COL1A1 knockdown via shRNA reduced COL1A1 levels in CM from both RXF-393 and CAKI-1 cells. In contrast, the COL1A1 could not be

detected in CM from RCC4 cells which have low basal *COL* expression (Fig. 6A, compare lane 5 with lanes 1 and 3). We therefore examined the effects of CM from high and low COL expressing RCC cells on SNAIL expression. RCC4 cells (low *COL* expression) cultured with the CM from CAKI-1 cells (high *COL* expression) demonstrated increased SNAIL1 protein relative to RCC4 cells incubated with CM from RCC4 cells (Fig. 6B). Correspondingly, RCC4 cells demonstrated enhanced migratory behavior when treated with CM from CAKI-1 cells (Fig. 6C). Furthermore, RCC4 cells cultured with the CM from COL1A1 knockdown (derived from CAKI-1 cells) had attenuated wound gap closure compared to the RCC4 cells incubated with the CM from shRNA control cells (fig. S5A–B). Based on these data, we determined whether extracellular collagen could promote migratory and invasive phenotypes. RCC4 cells (low basal *COL*) were cultured on a plate pre-coated with either collagen type I (COLI) or collagen type V (COLV) as well as an uncoated plate for 72 h. Both COLI and COLV treatment increased the expression of SNAIL1/2 proteins in RCC4 cells (Fig. 6D). Moreover, COLI and COLV treated RCC4 cells demonstrated significantly increased invasive and migratory properties (Fig. 6E and fig. S5C–D).

We next determined if extracellular *COL* produced by RCC cells could promote SNAIL accumulation. Immunodepletion was performed to remove COL1A1 protein from the CM of CAKI-1 cells as depicted in Fig. 6F. Immunoblotting of immunoprecipitates demonstrates successful pulldown of COL1A1 (fig. S5E). Correspondingly, immunodepleted media demonstrated reduced COL1A1 protein levels relative to IgG control pulldown media in CAKI-1 cells (Fig. 6G). RCC4 cells were then treated with COL1A1 immunodepleted CM and the corresponding IgG control treated CM. Notably, immunodepletion of COL1A1 from the CM of CAKI-1 cells resulted in decreased SNAIL1 protein (Fig. 6H). Collectively, these data indicate that extracellular collagen promotes SNAIL accumulation in RCC cells.

Given the role of extracellular collagen on SNAIL expression and invasive phenotypes, we examined the CM from PGC1α expressing RCC cells and found lower COL1A1 levels compared to the CM from control cells (Fig. 6I). We next considered the mechanism by which decreased collagen, via PGC1α, reduces SNAIL protein. Discoidin domain receptors (DDR1 and DDR2) are cell surface receptor tyrosine kinases known to bind collagen [12, 13]. Prior studies demonstrate that DDR2 activation can stabilize SNAIL1 protein in breast cancer [26]. The expression of DDRs was evaluated in renal tumors by RNA-seq data from the TCGA data set. Whereas *DDR1* was highly expressed in clear cell renal tumors, *DDR2* had very low expression (fig. S5F). Stable expression of COL1A1 in RCC4 cells induced phosphorylation of DDR1 and ERK, a downstream target of DDR1, without effects on total DDR1 and ERK (fig. S5G). Correspondingly, COL1A1 knockdown decreased phosphorylation of both DDR1 and ERK in CAKI-1 cells (Fig. 6J). Consistent with its role in regulating COL expression, PGC1α restoration decreased DDR1 and ERK phosphorylation in RCC cells (Fig. 6K). No effects on FAK phosphorylation were observed. Furthermore, treatment of RCC cells with the selective pharmacological DDR1 inhibitor 7rh decreased SNAIL1/2 protein in CAKI-1 cells in a dose-dependent manner (Fig. 6L). Taken together, these data indicate that PGC1α's suppression of *COL* expression leads to reduced DDR1 signaling, thereby promoting SNAIL degradation.

Discussion

Renal cancer is among the top ten most common malignancies in both men and women. Despite several approved agents, including immunotherapy and targeted therapies, metastatic ccRCC remains incurable and carries a poor prognosis. While the landscape of genetic alterations has been described in primary renal tumors [27, 28], less is understood about metastasis. As such, we undertook our current analysis to identify factors critical to RCC progression with the aim of identifying novel therapeutic targets.

Although PGC1α has been studied in cancer, its role in the context of metastasis has been inconsistent. PGC1α appears to suppress metastasis in prostate cancer [29], whereas PGC1α's bioenergetic activities promotes metastasis in breast cancer [30]. In a subset of melanomas, high PGC1α expression promotes growth and survival via its bioenergetics effects [31, 32]. Alternatively, PGC1α may suppress melanoma metastasis via activation of the transcription factor Inhibitor of DNA binding 2 (ID2) [33]. A recent study reported that PGC1α loss in ccRCC is mediated by HIF (which is elevated due to *VHL* mutation) and that restoration reduces proliferation and subcutaneous tumor xenograft growth [34]. We did not observe evidence of HIF-mediated suppression of PGC1α in our studies (data not shown). Effects of PGC1α on EMT, migration, or invasiveness were not examined. As *VHL* mutation is thought to be an early event in the majority of ccRCCs, our data demonstrating that PGC1α loss is associated with metastasis indicates that there are alternative mechanisms that suppress this factor which warrants further investigation.

Here, we provide two independent *in vivo* models to demonstrate the role of PGC1α in suppressing RCC tumor progression. To date, most of the studies examining PGC1α's role in metastasis suppression have been performed via intravenous injection. While these studies have been informative, they may more measure organ site colonization rather than true metastasis. These are the first data to demonstrate that PGC1α can mitigate tumor progression using an orthotopic tumor model which we believe is more representative of the metastatic process.

Prior studies on the role of PGC1α in cancer have linked phenotypes with PGC1α's bioenergetic function which is often mediated via interaction with ERRs. Torrano *et al.* recently reported that PGC1α's suppression of prostate cancer metastasis was ERR dependent [29]. We recently reported that ERRγ is epigenetically suppressed by methylation in RCC [14]. Here, we identify a completely novel role for PGC1α in tumor biology through the suppression of collagen expression that is ERR independent. The transcriptional regulation of collagen has been mainly described by transforming growth factor beta (TGF-β), a key enforcer of cancer progression through the modification of ECM in cancers [35, 36]. However, our data do not demonstrate that PGC1α impacts TGF-β signaling. Instead, PGC1α induces the expression of *miR-29a* which is known to target several *COL* genes [37, 38]. These data are in concert with recent studies indicating that *miR-29a* expression level is down-regulated in RCC tumors [39] and that restoration can suppresses migratory behaviors in RCC [19].

Collagens in tumor tissue have primarily been thought to be derived from stromal associated cells such as cancer-associated fibroblasts (CAFs). CAFs are commonly observed in stromal rich tumors including breast, pancreas, and lung [40–42]. In contrast, renal tumors have fewer CAFs in the microenvironment. Our *in vitro* characterization of RCC cell lines clearly demonstrates that a subset of RCC cell lines have higher expression of *COLs* in agreement with a recent study on *COL23* in RCC [11]. Furthermore, high COL expressing cell lines tended to have lower PGC1α expression with concomitant increased expression of SNAIL1 and SNAIL2. SNAILs have established roles in promoting invasive phenotypes in cancer cells. Our studies uncover an unexpected role for PGC1α in the regulation of SNAIL proteins. Mechanistically, PGC1α restoration suppresses collagen-mediated DDR1/ERK signaling which destabilizes SNAIL. Our studies indicate that this cascade, mediated by extracellular collagen, could impact signaling in high *COL* expressing cells as well as neighboring tumor cells which may have low *COL* expression. Therefore, these data have implications in the context of tumor heterogeneity in which cancer cells may have variable *COL* expression.

Collagens are the most abundant proteins and there are at least 28 different types of collagens identified so far. Based on their structure, they can be grouped into three major types: fibril-forming collagens, fibril-associated collagens with interrupted triple helices, and non-fibril-forming collagens [43]. Approximately 90% of collagen is characterized by the fibril-forming collagens including type I, V, and XI [44]. We found that these types of collagens are highly expressed in metastatic RCC and suppressed by the PGC1α/miR-29a axis. Collagens are known to interact with several different types of receptors, including receptor tyrosine kinases (RTKs). RTKs have clinical relevance to RCC since protein tyrosine kinase inhibitors are currently used in treatment of patients with metastatic ccRCC. The discoidin domain receptors, DDR1 and DDR2, are non-integrin collagen receptors that belong to the family of RTKs based on the presence of a catalytic kinase domain [45]. Recent studies have highlighted the different expression and mutation of DDRs in several types of cancers [46, 47]. DDR2 is known to stabilize SNAIL protein in the breast cancer [26], and DDR1 signaling enables metastatic breast cancer cells to undergo multi-organ metastases [48]. We found that DDR1 transcript levels are significantly higher in ccRCC compared to DDR2. Consistent with our data, a recent study reported that DDR1 expression is correlated with invasive behavior in RCC cells [49]; however, the downstream signaling events upon collagen/DDR1 interaction in RCC are poorly described. Here, we show that collagen in RCC cells activate the DDR1 and ERK axes to stabilize SNAIL1/2 proteins. In summary, our data provide new insight into the biologic basis of aggressive renal cancer and identify a novel link between PGC1α and the EMT promoters SNAIL1/2 vial collagen/DDR1 signaling (Fig. 7). The signaling cascade outlined may provide new opportunities for therapy given that many aspects of this signaling node are targetable.

Materials and Methods

Cell culture.

All RCC cell lines were acquired from the ATCC except for RXF-393 (NCI), RCC4 (kindly provided by P.Ratcliffe, University of Oxford), and SN12PM6-1 (kindly provided by Robert

S. Kerbel, University of Toronto). RCC cells RCC4, 786-O, A498, SN12PM6-1, and HEK293T cells were cultured in DMEM (Corning Life Science) with 10% fetal bovine serum (Hyclone) with penicillin-streptomycin (100U/mL). CAKI-1 and CAKI-2 cells were grown in MEM medium containing 10% FBS with antibiotics. RXF-393, 769-P, and OSRC2 cells were grown in RPMI medium. Cell lines were periodically screened for mycoplasma contamination.

Plasmid and virus infections.

Human PGC1α cDNA was purchased from GeneCopoeia. Human COL1A1 cDNA was purchased from Dharmacon. Lentiviral shRNA constructs for COL1A1 were purchased from Sigma. Lentiviral particles were produced by co-transfecting HEK293T cells with packaging plasmids (VSVG and Delta-8.9) using the calcium phosphate method. Virus-containing supernatants were collected after 48 hours and filtered through a 0.45 μm filter (Millipore). CAKI-1 and RXF-393 cells were infected with medium containing indicated virus in the presence of polybrene (8 μg/mL) (Sigma). Infected cells were selected with puromycin for 24 hours and surviving cells were maintained under puromycin selection. For transient expression of PGC1α, RCC cells were transduced with either GFP or PGC1α using adenovirus mediated gene transfer (Vector Biolabs).

Gene Expression Profiling.

The microarray experiment was conducted as recently reported in Nam *et. al.* [14]. The raw data and processed data have been uploaded in Gene expression Omnibus (GEO; #GSE105261).

TCGA gene expression correlation and outcome analysis.

Gene expression, correlation and survival analyses using TCGA clinical and level 3 RNA-seq data was performed using UALCAN web-portal [50].

siRNA transfection.

RCC4 cells were seeded on 6 well plates for 48 h. RCC4 cells were transfected with 50 nM of a negative control siRNA or siRNA against PGC1α using Lipofectamine® RNAiMAX regent (Invitrogen) for 48 h.

RNA isolation and Quantitative RT-PCR.

Total RNA from human tissues were isolated with the RNeasy Mini Kit (Qiagen). RNA from culture cells were extracted using the Trizol reagent (Ambion). cDNA was generated using a High-Capacity cDNA Reverse Transcription kit (Applied Biosystems). qRT-PCR analysis was followed using the Taqman Gene Expression Master reagent mixed Taqman primers with in QuantStudio™ 6K Flex Real-Time PCR System (Applied Biosystems). mRNA expression level was normalized to TATA-binding protein (TBP) and the normalized Ct value was quantified using the double delta Ct analysis. Indicated Taqman primers were pre-designed from Applied Biosystems (Table S2).

microRNA expression profiling.

RNA was extracted using mirVana™ miRNA isolation kit. The quality of the total RNA was verified by an Agilent 2100 Bioanalyzer. miRNA array profiling was processed as recommended by the manufacturer (NanoString Technologies Inc). The samples were processed on an nCounter Dx Prep Station and counted using an nCounter Dx Digital Analyzer (NanoString Technologies Inc). Differences in miRNA expression were assessed using the nSolver program (version 3.0).

MicroRNA and qRT-PCR.

Total RNA for miRNA expression were extracted using the mirVana™ miRNA isolation kit (ThermoFisher) according to the manufacturer's instructions. Reverse transcription was followed using a small RNA-specific stem-loop RT primer with Taqman MicroRNA Reverse Transcription kit (ThermoFisher). qRT-PCR analysis was performed using Taqman Universal PCR master mix II. For the inhibition of miR-29a, RCC cells were transfected for 48 h with 50 nM negative control or antagomiR-29a (ThermoFisher) using Lipofectamine® RNAiMAX reagent. For the induction of miR-29a, RCC cells were transiently transfected with 50 nM negative control or miR-29a mimics (ThermoFisher). Relative miRNA expression was determined using the $2^{-\Delta\Delta ct}$ with human U6 snRNA as the internal reference gene.

Collagen coating of tissue culture surfaces.

Collagen type I from calf skin (Sigma) and collagen type V from human placenta (Sigma) were reconstituted with 0.02 M acetic acid for 2 h. The diluted collagen solution (5 ug/cm^2) was coated on a 6 well plate for 1 h at room temperature. The excess diluted collagen solution was aspirated, and the plate rinsed with PBS before seeding RCC4 cells.

Immunoblotting analysis.

Cells were lysed with ice-cold RIPA buffer containing 1X protease inhibitor. Human kidney tissue was homogenized using microbeads (Bioexpress). Preparation of samples and Western blot analyses were described previously [14]. Nuclear extraction for PGC1α detection was performed using a commercial kit (Pierce). Antibodies used in this study are described in Table S2. The full uncut images for each blot are provided in fig. S6.

Immunoprecipitation.

The conditioned media from CAKI-1 cells were incubated with either total 5 ug of COL1A1 or IgG antibody coated with A/G magnetic beads (ThermoFisher) for overnight at 4 ° with rotation. The immune complex was then filtered and washed three times with 20 mM Tris-HCl, 150 mM NaCl, 2 mM EDTA (pH 8.0). The immunoprecipitated proteins were eluted by boiling beads in Laemmli buffer and analyzed by immunoblot analysis.

Wound healing and migration assay.

RCC cells were seeded on 6 well plates to reach 90% confluence and then mechanically disrupted using 1000μl pipette tips. Cell migration was monitored with an EVOS™ FL imaging system (Invitrogen) at the indicated times. For the transwell migration assay, cells

were seeded in serum-free medium onto the upper chamber of the transwell insert (Corning) for 24 h. The migrated cells were fixed and quantified by crystal violet staining.

Matrigel-based invasion assay.

RCC cells were plated on the upper chambers of a BD BioCoat Matrigel Matrix (Corning). The cells were allowed to invade through the Matrigel layer for 16 h and then stained with Diff-Quik Stain kit (Siemens). Invading cells were counted under a light microscope.

Isolation of Non-invasive versus invasive cells.

RCC cells were plated on the upper chambers of BD BioCoat Matrigel Matrix (Corning) for 24 h. The non-invasive cells were harvested using a Corning Cell Recovery Solution following the manufacturer's instructions. The non-invasive cells were resuspended using a lysis buffer in the Cells-to-cDNA II kit (Invitrogen). The invasive cells on the bottom of membrane were directly collected by a lysis buffer in the Cells-to-cDNA II kit (Invitrogen).

Chick chorioallantoic membrane assay.

CAM assay was performed according to the previously described method with slight modifications [51]. Briefly, specific pathogen free fertile eggs (Charles River Laboratories) were incubated in a rotary humidified chamber (60~65%) for 10 days. Two million cells were resuspended in media and mixed with an equal volume of BD Matrigel Basement Membrane Matrix (Corning). Approximately 2 million RXF-393 cells were implanted on the upper CAM of 10-day old chick embryos after creating a small window in the egg shell which was subsequently sealed. On the 17^{th} day of the experiment, the lungs and liver were harvested, and genomic DNA was isolated using a Wizard genomic DNA isolation kit (Promega). Quantification of the invaded tumor cells was performed with a Taqman-based ALU assay.

Orthotopic tumor challenge and xenograft study.

Tumor challenges were performed using 5 weeks old SCID male mice. A skin incision was made and SN12PM6-1 ($1\times10\text{^}6$) cells were injected through the intact peritoneum into the left kidney. Bioluminescent imaging was performed weekly, and mice were sacrificed 6 weeks later.

Data analysis and statistics.

Data are represented as mean ± SEM of at least 3 independent experiments. The exact number of samples is described in the corresponding figure legend. Tests of statistical significance between control and experimental groups were performed using Student's *t* test or a 1-way ANOVA. *p* values of less than 0.05 were considered statistically significant.

Study approval.

Fresh frozen normal kidney and tumor tissues were obtained in accordance with an IRB-approved protocol. All animal studies were performed following approval from the institutional IACUC.

Supplementary Material

Refer to Web version on PubMed Central for supplementary material.

Acknowledgements

This work was supported by Department of Veteran Affairs grant BX002930 and NCI R01 CA200653 (S.S). Research reported in this publication was also supported by the NIH (P30 CA013148). The funders had no role in study design, data collection and analysis, decision to publish, or preparation of the manuscript. There are no conflicts of interest. We would like to acknowledge Eddy Yang and Debbie Della Manna for assistance with miRNA profiling. Array data were generated by the UT Health San Antonio Cancer Center Genomics Shared Resource.

References

[1]. Siegel RL, Miller KD, Jemal A, Cancer statistics, 2016, CA: a cancer journal for clinicians 66(1) (2016) 7–30. [PubMed: 26742998]

[2]. Gnarra JR, Tory K, Weng Y, Schmidt L, Wei MH, Li H, Latif F, Liu S, Chen F, Duh FM, et al., Mutations of the VHL tumour suppressor gene in renal carcinoma, Nature genetics 7(1) (1994) 85–90. [PubMed: 7915601]

[3]. Finck BN, Kelly DP, PGC-1 coactivators: inducible regulators of energy metabolism in health and disease, J Clin Invest 116(3) (2006) 615–22. [PubMed: 16511594]

[4]. Handschin C, Spiegelman BM, The role of exercise and PGC1alpha in inflammation and chronic disease, Nature 454(7203) (2008) 463–9. [PubMed: 18650917]

[5]. Lin J, Handschin C, Spiegelman BM, Metabolic control through the PGC-1 family of transcription coactivators, Cell Metab 1(6) (2005) 361–70. [PubMed: 16054085]

[6]. Haemmerle G, Moustafa T, Woelkart G, Buttner S, Schmidt A, van de Weijer T, Hesselink M, Jaeger D, Kienesberger PC, Zierler K, Schreiber R, Eichmann T, Kolb D, Kotzbeck P, Schweiger M, Kumari M, Eder S, Schoiswohl G, Wongsiriroj N, Pollak NM, Radner FP, Preiss-Landl K, Kolbe T, Rulicke T, Pieske B, Trauner M, Lass A, Zimmermann R, Hoefler G, Cinti S, Kershaw EE, Schrauwen P, Madeo F, Mayer B, Zechner R, ATGL-mediated fat catabolism regulates cardiac mitochondrial function via PPAR-alpha and PGC-1, Nat Med 17(9) (2011) 1076–85. [PubMed: 21857651]

[7]. Mammoto T, Ingber DE, Mechanical control of tissue and organ development, Development 137(9) (2010) 1407–20. [PubMed: 20388652]

[8]. Cen L, Liu W, Cui L, Zhang W, Cao Y, Collagen tissue engineering: development of novel biomaterials and applications, Pediatr Res 63(5) (2008) 492–6. [PubMed: 18427293]

[9]. Frantz C, Stewart KM, Weaver VM, The extracellular matrix at a glance, J Cell Sci 123(Pt 24) (2010) 4195–200. [PubMed: 21123617]

[10]. Gewin LS, Renal fibrosis: Primacy of the proximal tubule, Matrix Biol 68–69 (2018) 248–262.

[11]. Xu F, Chang K, Ma J, Qu Y, Xie H, Dai B, Gan H, Zhang H, Shi G, Zhu Y, Zhu Y, Shen Y, Ye D, The Oncogenic Role of COL23A1 in Clear Cell Renal Cell Carcinoma, Scientific reports 7(1) (2017) 9846. [PubMed: 28852123]

[12]. Shrivastava A, Radziejewski C, Campbell E, Kovac L, McGlynn M, Ryan TE, Davis S, Goldfarb MP, Glass DJ, Lemke G, Yancopoulos GD, An orphan receptor tyrosine kinase family whose members serve as nonintegrin collagen receptors, Molecular cell 1(1) (1997) 25–34. [PubMed: 9659900]

[13]. Vogel W, Gish GD, Alves F, Pawson T, The discoidin domain receptor tyrosine kinases are activated by collagen, Molecular cell 1(1) (1997) 13–23. [PubMed: 9659899]

[14]. Nam HY, Chandrashekar DS, Kundu A, Shelar S, Kho EY, Sonpavde G, Naik G, Ghatalia P, Livi CB, Varambally S, Sudarshan S, Integrative Epigenetic and Gene Expression Analysis of Renal Tumor Progression to Metastasis, Mol Cancer Res 17(1) (2019) 84–96. [PubMed: 30131446]

[15]. Pakshir P, Hinz B, The big five in fibrosis: Macrophages, myofibroblasts, matrix, mechanics, and miscommunication, Matrix Biol 68–69 (2018) 81–93.

[16]. Charest-Marcotte A, Dufour CR, Wilson BJ, Tremblay AM, Eichner LJ, Arlow DH, Mootha VK, Giguere V, The homeobox protein Prox1 is a negative modulator of ERR{alpha}/PGC-1{alpha} bioenergetic functions, Genes Dev 24(6) (2010) 537–42. [PubMed: 20194433]

[17]. Castoldi G, Di Gioia CR, Bombardi C, Catalucci D, Corradi B, Gualazzi MG, Leopizzi M, Mancini M, Zerbini G, Condorelli G, Stella A, MiR-133a regulates collagen 1A1: potential role of miR-133a in myocardial fibrosis in angiotensin II-dependent hypertension, J Cell Physiol 227(2) (2012) 850–6. [PubMed: 21769867]

[18]. Ji J, Zhao L, Budhu A, Forgues M, Jia HL, Qin LX, Ye QH, Yu J, Shi X, Tang ZY, Wang XW, Let-7g targets collagen type I alpha2 and inhibits cell migration in hepatocellular carcinoma, J Hepatol 52(5) (2010) 690–7. [PubMed: 20338660]

[19]. Nishikawa R, Chiyomaru T, Enokida H, Inoguchi S, Ishihara T, Matsushita R, Goto Y, Fukumoto I, Nakagawa M, Seki N, Tumour-suppressive microRNA-29s directly regulate LOXL2 expression and inhibit cancer cell migration and invasion in renal cell carcinoma, FEBS Lett 589(16) (2015) 2136–45. [PubMed: 26096783]

[20]. Jedeszko C, Paez-Ribes M, Di Desidero T, Man S, Lee CR, Xu P, Bjarnason GA, Bocci G, Kerbel RS, Postsurgical adjuvant or metastatic renal cell carcinoma therapy models reveal potent antitumor activity of metronomic oral topotecan with pazopanib, Sci Transl Med 7(282) (2015) 282ra50.

[21]. Thiery JP, Acloque H, Huang RY, Nieto MA, Epithelial-mesenchymal transitions in development and disease, Cell 139(5) (2009) 871–90. [PubMed: 19945376]

[22]. Yook JI, Li XY, Ota I, Fearon ER, Weiss SJ, Wnt-dependent regulation of the E-cadherin repressor snail, J Biol Chem 280(12) (2005) 11740–8. [PubMed: 15647282]

[23]. Fu HL, Valiathan RR, Arkwright R, Sohail A, Mihai C, Kumarasiri M, Mahasenan KV, Mobashery S, Huang P, Agarwal G, Fridman R, Discoidin domain receptors: unique receptor tyrosine kinases in collagen-mediated signaling, J Biol Chem 288(11) (2013) 7430–7. [PubMed: 23335507]

[24]. Jokinen J, Dadu E, Nykvist P, Kapyla J, White DJ, Ivaska J, Vehvilainen P, Reunanen H, Larjava H, Hakkinen L, Heino J, Integrin-mediated cell adhesion to type I collagen fibrils, J Biol Chem 279(30) (2004) 31956–63. [PubMed: 15145957]

[25]. Leitinger B, Transmembrane collagen receptors, Annu Rev Cell Dev Biol 27 (2011) 265–90. [PubMed: 21568710]

[26]. Zhang K, Corsa CA, Ponik SM, Prior JL, Piwnica-Worms D, Eliceiri KW, Keely PJ, Longmore GD, The collagen receptor discoidin domain receptor 2 stabilizes SNAIL1 to facilitate breast cancer metastasis, Nature cell biology 15(6) (2013) 677–87. [PubMed: 23644467]

[27]. Brugarolas J, Molecular genetics of clear-cell renal cell carcinoma, J Clin Oncol 32(18) (2014) 1968–76. [PubMed: 24821879]

[28]. Cancer N. Genome Atlas Research, Comprehensive molecular characterization of clear cell renal cell carcinoma, Nature 499(7456) (2013) 43–9. [PubMed: 23792563]

[29]. Torrano V, Valcarcel-Jimenez L, Cortazar AR, Liu X, Urosevic J, Castillo-Martin M, Fernandez-Ruiz S, Morciano G, Caro-Maldonado A, Guiu M, Zuniga-Garcia P, Graupera M, Bellmunt A, Pandya P, Lorente M, Martin-Martin N, Sutherland JD, Sanchez-Mosquera P, Bozal-Basterra L, Zabala-Letona A, Arruabarrena-Aristorena A, Berenguer A, Embade N, Ugalde-Olano A, Lacasa-Viscasillas I, Loizaga-Iriarte A, Unda-Urzaiz M, Schultz N, Aransay AM, Sanz-Moreno V, Barrio R, Velasco G, Pinton P, Cordon-Cardo C, Locasale JW, Gomis RR, Carracedo A, The metabolic co-regulator PGC1alpha suppresses prostate cancer metastasis, Nature cell biology 18(6) (2016) 645–656. [PubMed: 27214280]

[30]. LeBleu VS, O'Connell JT, Gonzalez Herrera KN, Wikman H, Pantel K, Haigis MC, de Carvalho FM, Damascena A, Domingos Chinen LT, Rocha RM, Asara JM, Kalluri R, PGC-1alpha mediates mitochondrial biogenesis and oxidative phosphorylation in cancer cells to promote metastasis, Nature cell biology 16(10) (2014) 992–1003, 1–15. [PubMed: 25241037]

[31]. Haq R, Shoag J, Andreu-Perez P, Yokoyama S, Edelman H, Rowe GC, Frederick DT, Hurley AD, Nellore A, Kung AL, Wargo JA, Song JS, Fisher DE, Arany Z, Widlund HR, Oncogenic BRAF regulates oxidative metabolism via PGC1alpha and MITF, Cancer Cell 23(3) (2013) 302–15. [PubMed: 23477830]

[32]. Vazquez F, Lim JH, Chim H, Bhalla K, Girnun G, Pierce K, Clish CB, Granter SR, Widlund HR, Spiegelman BM, Puigserver P, PGC1alpha expression defines a subset of human melanoma tumors with increased mitochondrial capacity and resistance to oxidative stress, Cancer Cell 23(3) (2013) 287–301. [PubMed: 23416000]

[33]. Luo C, Lim JH, Lee Y, Granter SR, Thomas A, Vazquez F, Widlund HR, Puigserver P, A PGC1alpha-mediated transcriptional axis suppresses melanoma metastasis, Nature 537(7620) (2016) 422–426. [PubMed: 27580028]

[34]. LaGory EL, Wu C, Taniguchi CM, Ding CC, Chi JT, von Eyben R, Scott DA, Richardson AD, Giaccia AJ, Suppression of PGC-1alpha Is Critical for Reprogramming Oxidative Metabolism in Renal Cell Carcinoma, Cell Rep 12(1) (2015) 116–127. [PubMed: 26119730]

[35]. Massague J, TGFbeta in Cancer, Cell 134(2) (2008) 215–30. [PubMed: 18662538]

[36]. Gyorfi AH, Matei AE, Distler JHW, Targeting TGF-beta signaling for the treatment of fibrosis, Matrix Biol 68–69 (2018) 8–27.

[37]. Kwiecinski M, Noetel A, Elfimova N, Trebicka J, Schievenbusch S, Strack I, Molnar L, von Brandenstein M, Tox U, Nischt R, Coutelle O, Dienes HP, Odenthal M, Hepatocyte growth factor (HGF) inhibits collagen I and IV synthesis in hepatic stellate cells by miRNA-29 induction, PLoS One 6(9) (2011) e24568.

[38]. van Rooij E, Sutherland LB, Thatcher JE, DiMaio JM, Naseem RH, Marshall WS, Hill JA, Olson EN, Dysregulation of microRNAs after myocardial infarction reveals a role of miR-29 in cardiac fibrosis, Proc Natl Acad Sci U S A 105(35) (2008) 13027–32. [PubMed: 18723672]

[39]. He H, Wang L, Zhou W, Zhang Z, Wang L, Xu S, Wang D, Dong J, Tang C, Tang H, Yi X, Ge J, MicroRNA Expression Profiling in Clear Cell Renal Cell Carcinoma: Identification and Functional Validation of Key miRNAs, PLoS One 10(5) (2015) e0125672.

[40]. Chen L, Qu C, Chen H, Xu L, Qi Q, Luo J, Wang K, Meng Z, Chen Z, Wang P, Liu L, Chinese herbal medicine suppresses invasion-promoting capacity of cancer-associated fibroblasts in pancreatic cancer, PLoS One 9(4) (2014) e96177.

[41]. Gorchs L, Hellevik T, Bruun JA, Camilio KA, Al-Saad S, Stuge TB, Martinez-Zubiaurre I, Cancer-associated fibroblasts from lung tumors maintain their immunosuppressive abilities after high-dose irradiation, Front Oncol 5 (2015) 87. [PubMed: 26029659]

[42]. Hosein AN, Livingstone J, Buchanan M, Reid JF, Hallett M, Basik M, A functional in vitro model of heterotypic interactions reveals a role for interferon-positive carcinoma associated fibroblasts in breast cancer, BMC Cancer 15 (2015) 130. [PubMed: 25884794]

[43]. Gelse K, Poschl E, Aigner T, Collagens--structure, function, and biosynthesis, Adv Drug Deliv Rev 55(12) (2003) 1531–46. [PubMed: 14623400]

[44]. Lodish H BA, Zipursky SL, et al., Collagen:The Fibrous Proteins of the Matrix, 4th edition ed., Freeman WH, New York, 2000.

[45]. Alves F, Vogel W, Mossie K, Millauer B, Hofler H, Ullrich A, Distinct structural characteristics of discoidin I subfamily receptor tyrosine kinases and complementary expression in human cancer, Oncogene 10(3) (1995) 609–18. [PubMed: 7845687]

[46]. Ford CE, Lau SK, Zhu CQ, Andersson T, Tsao MS, Vogel WF, Expression and mutation analysis of the discoidin domain receptors 1 and 2 in non-small cell lung carcinoma, Br J Cancer 96(5) (2007) 808–14. [PubMed: 17299390]

[47]. Valiathan RR, Marco M, Leitinger B, Kleer CG, Fridman R, Discoidin domain receptor tyrosine kinases: new players in cancer progression, Cancer Metastasis Rev 31(1–2) (2012) 295–321. [PubMed: 22366781]

[48]. Gao H, Chakraborty G, Zhang Z, Akalay I, Gadiya M, Gao Y, Sinha S, Hu J, Jiang C, Akram M, Brogi E, Leitinger B, Giancotti FG, Multi-organ Site Metastatic Reactivation Mediated by Non-canonical Discoidin Domain Receptor 1 Signaling, Cell 166(1) (2016) 47–62. [PubMed: 27368100]

[49]. Song J, Chen X, Bai J, Liu Q, Li H, Xie J, Jing H, Zheng J, Discoidin domain receptor 1 (DDR1), a promising biomarker, induces epithelial to mesenchymal transition in renal cancer cells, Tumour Biol 37(8) (2016) 11509–21. [PubMed: 27020590]

[50]. Chandrashekar DS, Bashel B, Balasubramanya SAH, Creighton CJ, Ponce-Rodriguez I, Chakravarthi B, Varambally S, UALCAN: A Portal for Facilitating Tumor Subgroup Gene Expression and Survival Analyses, Neoplasia (New York, N.Y 19(8) (2017) 649–658.

[51]. Chakravarthi BV, Goswami MT, Pathi SS, Robinson AD, Cieslik M, Chandrashekar DS, Agarwal S, Siddiqui J, Daignault S, Carskadon SL, Jing X, Chinnaiyan AM, Kunju LP, Palanisamy N, Varambally S, MicroRNA-101 regulated transcriptional modulator SUB1 plays a role in prostate cancer, Oncogene 35(49) (2016) 6330–6340. [PubMed: 27270442]

Highlights

- The decreased expression of PGC1α and the increased expression of several collagen genes are associated with progression of renal cell carcinoma (RCC).
- Restoration of PGC1α in RCC cells suppresses the expression of collagens and tumor phenotypes via the induction of *miR-29a* as well as tumor progression *in vivo*.
- The suppression of collagens by PGC1α/*miR-29a* axis promotes the degradation of the known EMT regulators SNAIL1 and SNAIL2, which promote cancer invasiveness.

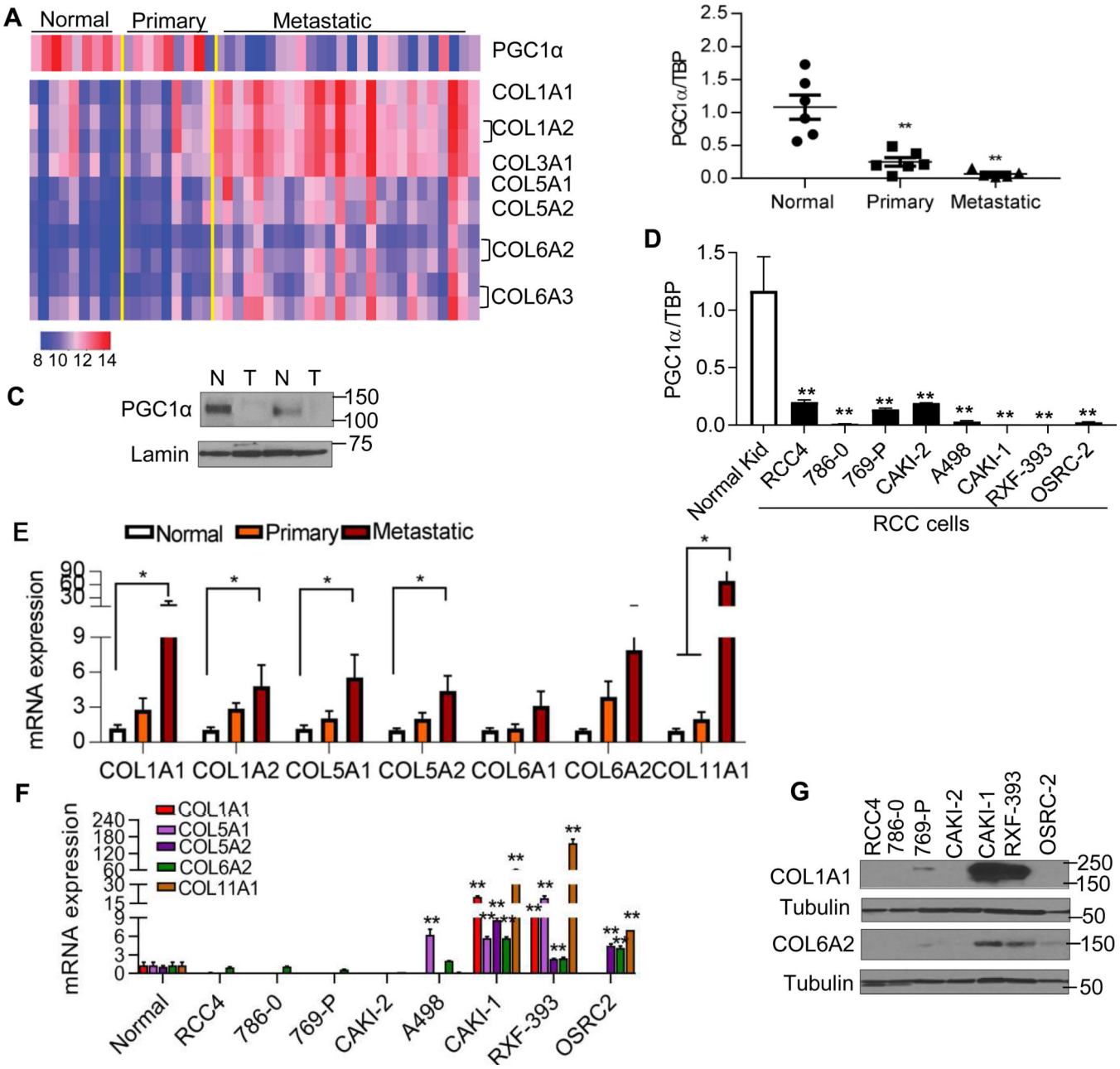

Fig. 1. Gene expression signatures of tumor progression in RCC

(**A**) Heatmap representing expression patterns of *PGC1α* and collagen family members (*COLs*) using the Illumina Human HT-12 v4 bead array in the three-patient groups (normal n=9, primary n=9, and metastasis n=26). Colors in the heatmap represent log transformed quantile normalized expression values for selected set of probes in individual samples. Normalized expression values for probes of selected genes ranged between 8 and 14. Specifically, high expression values indicated in red and low expression values indicated in blue. (**B**) Quantitative RT-PCR analysis of *PGC1α* expression in a separate cohort of patient-matched samples. Transcript levels were normalized to those of *TBP* (n=6/group). (**C**) Immunoblot analysis of PGC1α in patient-matched normal kidney (N) and tumor (T). (**D**)

Relative mRNA expression of *PGC1α* in a panel of RCC cell lines compared to primary normal kidney tissue (n=4/group). (**E**) Relative mRNA expression of *COLs* in a separate cohort of patient-matched normal, primary, and metastatic tumor deposits. (**F**) Relative mRNA expression of *COLs* in a panel of RCC cell lines compared to primary normal kidney tissue (n=4/group). (**G**) Western blot analysis of COL1A1 and COL6A2 in a panel of RCC cell lines. All data represent 3 independent experiments and error bars are SEM. Asterisks indicate significant differences compared to normal kidney (*P<0.05, **P<0.01, One-way ANOVA with Tukey's multiple comparisons test).

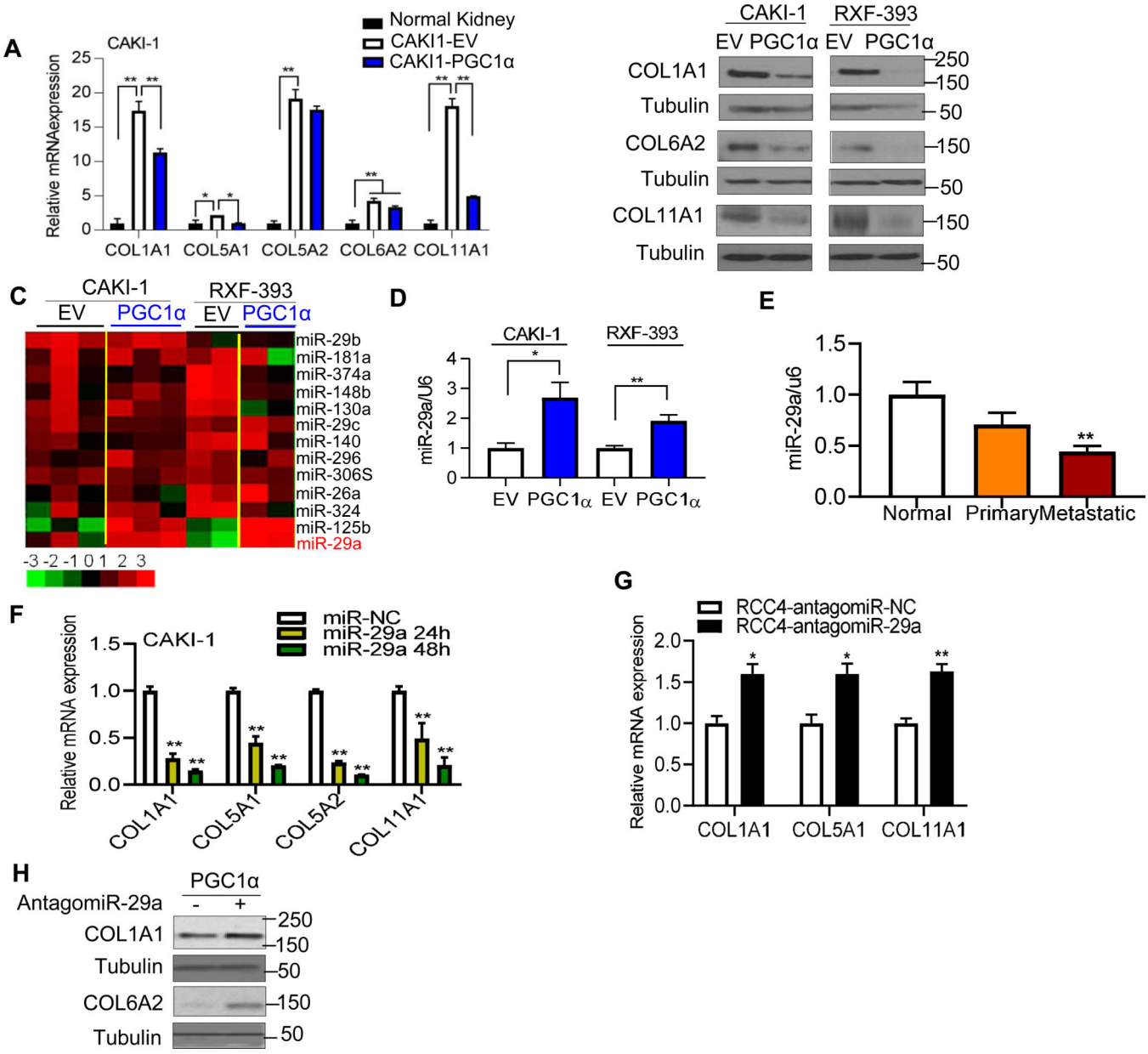

Fig. 2. PGC1α inhibits the expression of collagens in a miR-29a dependent manner.

(**A**) Relative mRNA expression of *COLs* in stable CAKI-1 cells expressing an EV or PGC1α compared to normal kidney (n=3/group, 3 independent experiments). (**B**) Western blot analysis of COL1A1, COL6A2, and COL11A1 in CAKI-1 and RXF-393 cells stably expressing an EV or PGC1α. (**C**) Heatmap of miRNA profile in RCC cells stably expressing an EV or PGC1α using a NanoString miRNA assay (n=2~3/group). (**D**) Relative *miR-29a* expression in stable CAKI-1 and RXF-393 cells expressing an EV or PGC1α. U6 snRNA was used for normalization (n=3/group). (**E**) Relative *miR-29a* expression in a separate cohort of patient-matched normal, primary, and metastatic tumor deposits (n=5/group). (**F**) CAKI-1 cells were transfected with either 50 nM negative control (NC) or synthetic miR-29a mimic for the indicated times. The mRNA expression of *COLs* was analyzed by

qRT-PCR (n=3/group). (**G**) RCC4 cells were transfected with either 50 nM antagomiR-NC (negative control) or antagomiR-29a for 24 h. (**H**) Western blot analysis of COL1A1 and COL6A2 in PGC1α-expressing CAKI-1 cells after transfection with either 50 nM antagomiR-NC or antigomiR-29a for 48 hr. All data represent 3 independent experiments and error bars are SEM. Asterisks indicate significant differences compared to control cells (*P<0.05, **P<0.01, One-way ANOVA with Tukey's multiple comparisons test or 2 tailed student t test).

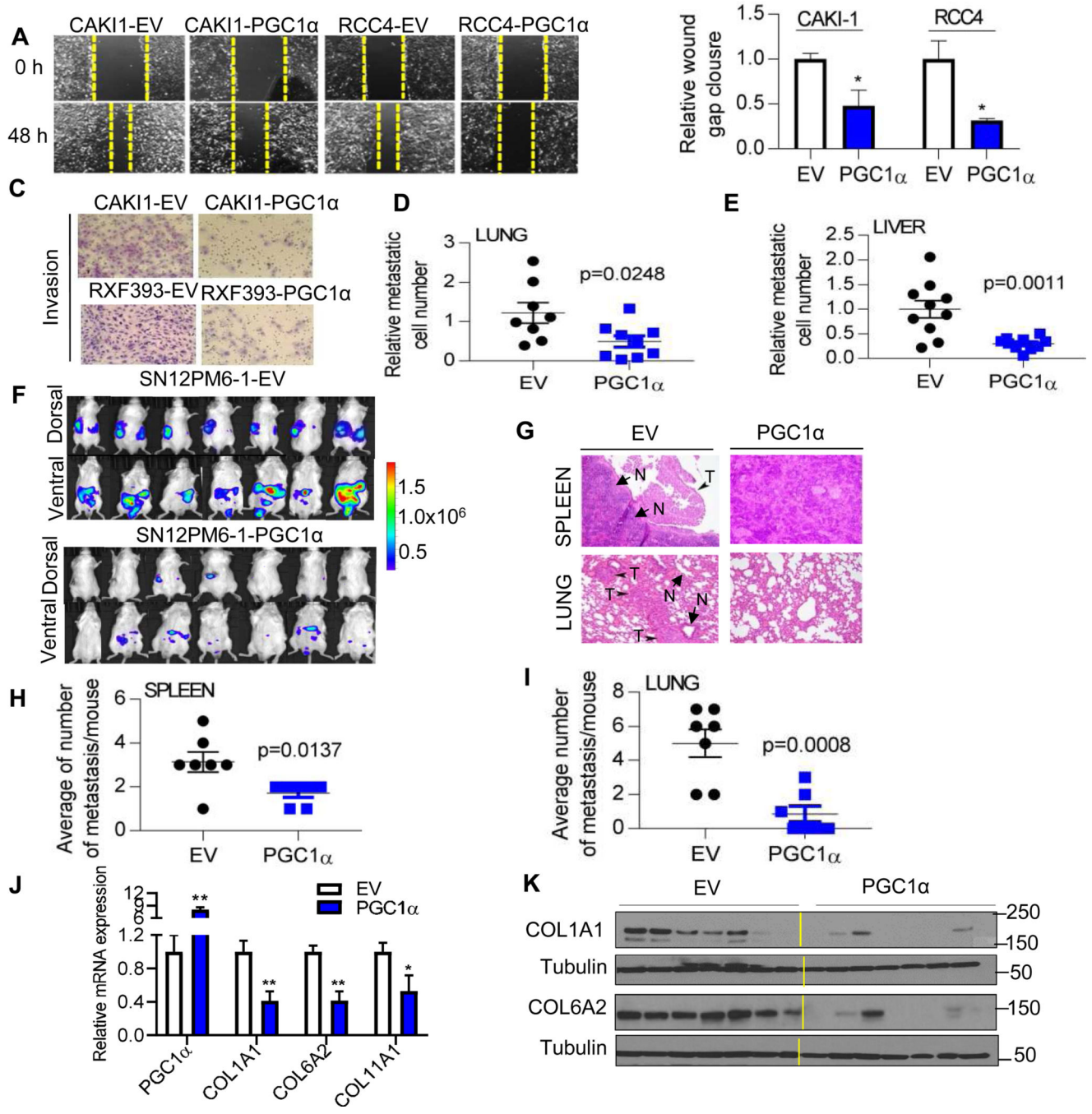

Fig. 3. PGC1α suppresses the migratory and invasive phenotypes of ccRCC cells.

(**A**) Representative images and (**B**) relative wound healing over time in RCC cells (n=3/group). (**C**) Representative images of Boyden invasion assay with Matrigel insert in RCC cells. (n=3/group). (**D and E**) Chick embryo chorioallantoic membrane (CAM) metastasis assay. Two million RXF393 cells were implanted on the upper CAM vessels of 10-day old chick embryos. One week later, tissues were harvested and metastasis of RCC cells was quantified by qPCR of human Alu repeats in genomic DNA (n=10/group). (**F**) Bioluminescence *in vivo* imaging at 6 weeks after tumor challenge. SN12PM6-1 cells were

orthotopically implanted into the left kidney of SCID mice (n=7/group). (**G**) H&E staining of tissue sections from the mice orthotopically implanted with an EV or PGC1α expressing SN12PM6-1 cells at 6-week after tumor challenge. Arrows indicate metastatic tumors (T) and normal tissues (N). Spontaneous metastasis to the spleen (**H**) and lung (**I**) was quantified. (**J**) At 6 weeks from tumor challenge, kidney tumors were harvested and analyzed for the mRNA expression of *PGC1α* and *COLs* (n=7/group). (**K**) COL1A1 and COL6A2 protein levels in kidney tumors from the mice orthotopically implanted with an EV or PGC1α expressing SN12PM6-1 cells (n=7/group).

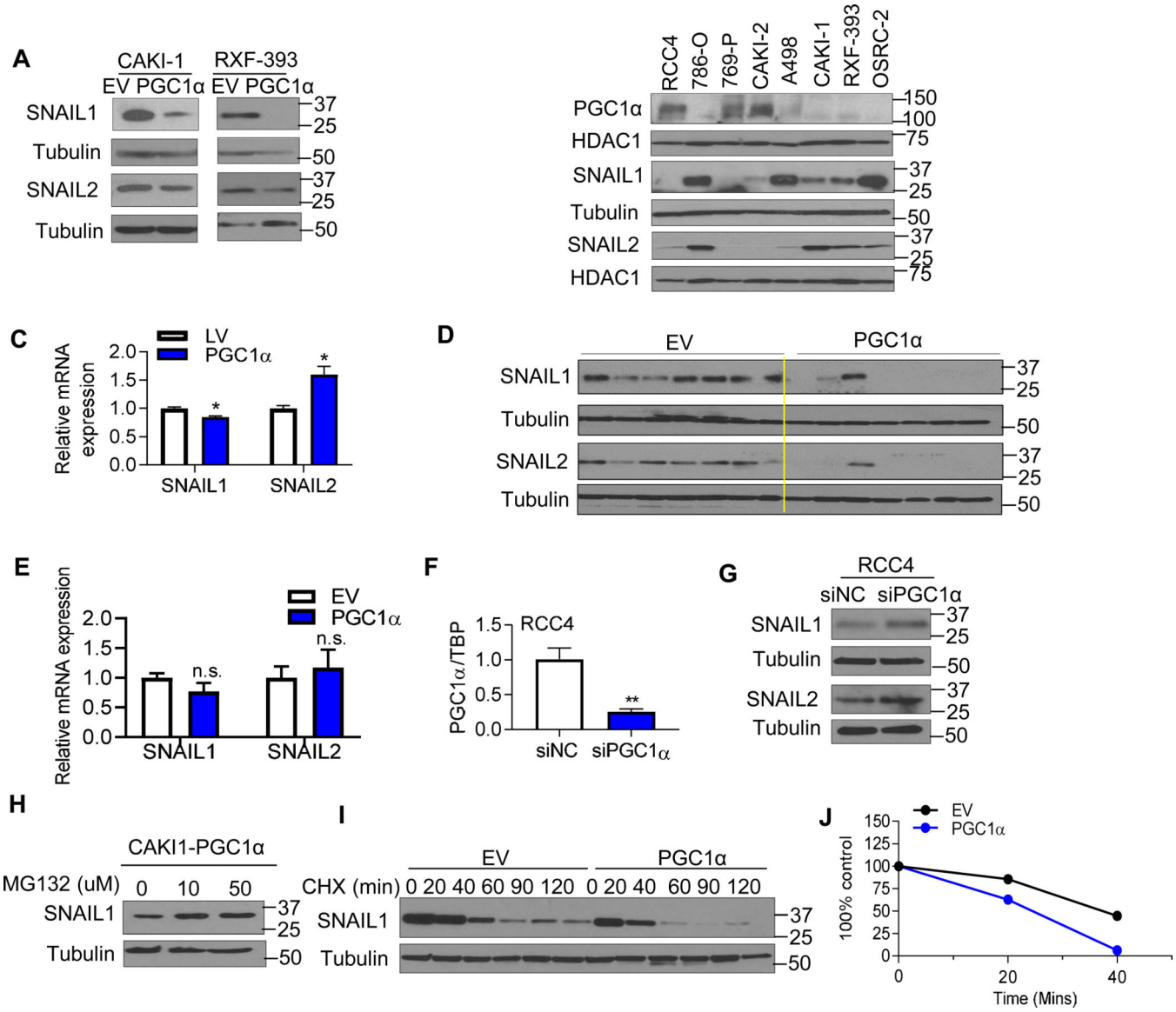

Fig. 4. PGC1α destabilizes the SNAIL protein in ccRCC.

(**A**) Western blot analysis of SNAIL1 and SNAIL2 in the stable CAKI-1 and RXF-393 cells expressing an EV or PGC1α. (**B**) Immunoblot analysis of PGC1α, SNAIL1, and SNAIL2 in a panel of RCC cell lines. HDAC1 was used to normalize protein loading. (**C**) Relative mRNA expression of SNAIL1 and SNAIL2 in stable CAKI-1 cells expressing an EV or PGC1α (n=3/group). TBP was used as normalizing control for gene expression. (**D**) At 6 weeks from tumor challenge, kidney tumors were harvested and analyzed for the expression of SNAIL1 and SNAIL2 (n=7/group). (**E**) Relative mRNA expression of SNAIL1/2 in dissected kidneys injected tumors cells at 6 weeks from tumor challenge (n=7/group). (**F**) Relative mRNA expression of *PGC1α* in RCC4 cells transfected with either 50 nM negative control siRNA (NC) or PGC1α siRNA for 48 hr (***P*<0.01, 2 tail student *t* test). (**G**) Western blot analysis of SNAIL1 and SNAIL2 in RCC4 cells transfected with either 50 nM NC or PGC1α siRNA for 48 hr. (**H**) Stable PGC1α expressing CAKI-1 cells were treated

with the indicated concentration of proteasome inhibitor MG132 for 4 hr. SNAIL1 protein levels were analyzed by immunoblot analysis. (**I**) CAKI-1 cells stably expressing an EV or PGC1α were incubated with 10 μg/ml cycloheximide (CHX) for the indicated times. Cell lysates were immunoblotted with SNAIL1 and tubulin antibodies. (**J**) Immunoblot analysis of SNAIL as shown in (I) was quantified using Image J program. All data represent 3 independent experiments and error bars are SEM (*P<0.05, **P<0.01, 2 tail student t test).

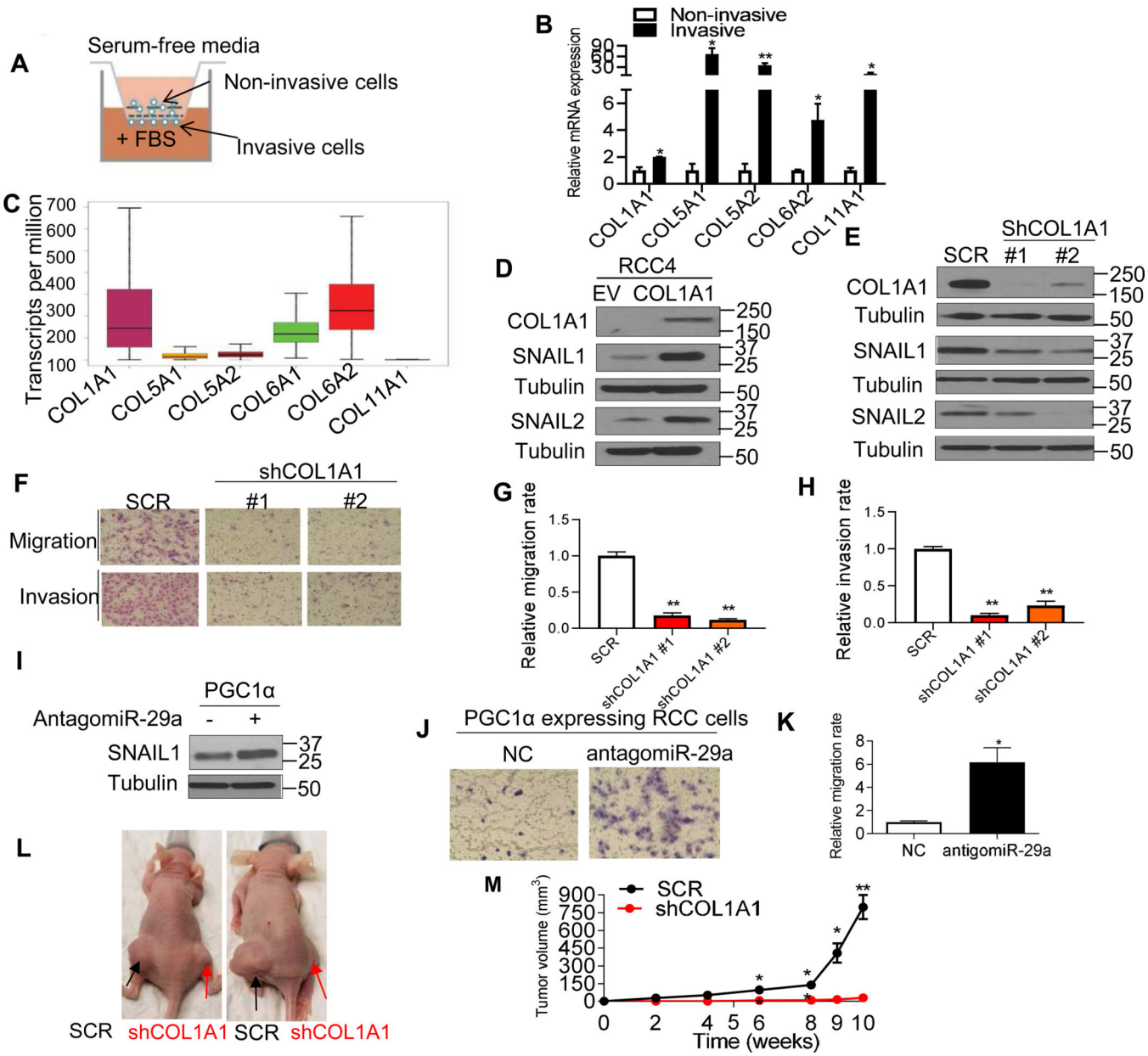

Fig. 5. COL1A1 knockdown diminishes the migratory and invasive phenotype in ccRCC.

(A) Schematic diagram representing the isolation of non-invasive and invasive cells using a Boyden invasion chamber with Matrigel insert. CAKI-1 cells were seeded in the chambers for 24 h. The non-invasive cells from inside of the chamber as well as invasive cells from the bottom of the membrane were separately harvested. (**B**) Relative mRNA expression of *COLs* in invasive cells relative to non-invasive cells. 18S used as a housekeeping gene (n=3/group). (**C**) RNA-Seq analysis of gene expression for *COLs* in the renal tumors in the TCGA data set. (**D**) Western blot analysis of the indicated proteins in RCC4 cells stably expressing an EV or *COL1A1* cDNA. (**E**) Western blot analysis of the indicated proteins in CAKI-1 cells stably expressing shRNA control (SCR) or two independent *COL1A1* shRNA constructs. (**F**) Representative images and (**G and H**) quantification of migratory and invasive

phenotype in CAKI-1 cells. (**I**) Western blot analysis of SNAIL1 in PGC1α-expressing CAKI-1 cells after transfection with either NC or antigomiR-29a for 48 hr. (**J**) Representative images and (**K**) relative quantification of Transwell migration assay in CAKI-1 cells stably expressing PGC1α after transfection with NC or antigo*miR-29a* for 48 h (n=3/group). (**L**) Representative images of nude mice showing tumor growth of CAKI-1 cells. Two million CAKI-1 cells stably expressing SCR or *COL1A1* shRNA were subcutaneously injected into the flanks of female BALB/c nu/nu mice at 5–7 weeks old (n=6/group). (**M**) Caliper measurements of the tumor volumes were taken on the indicated weeks. All data are presented as mean ± SEM (**P*<0.05, ***P*<0.01).

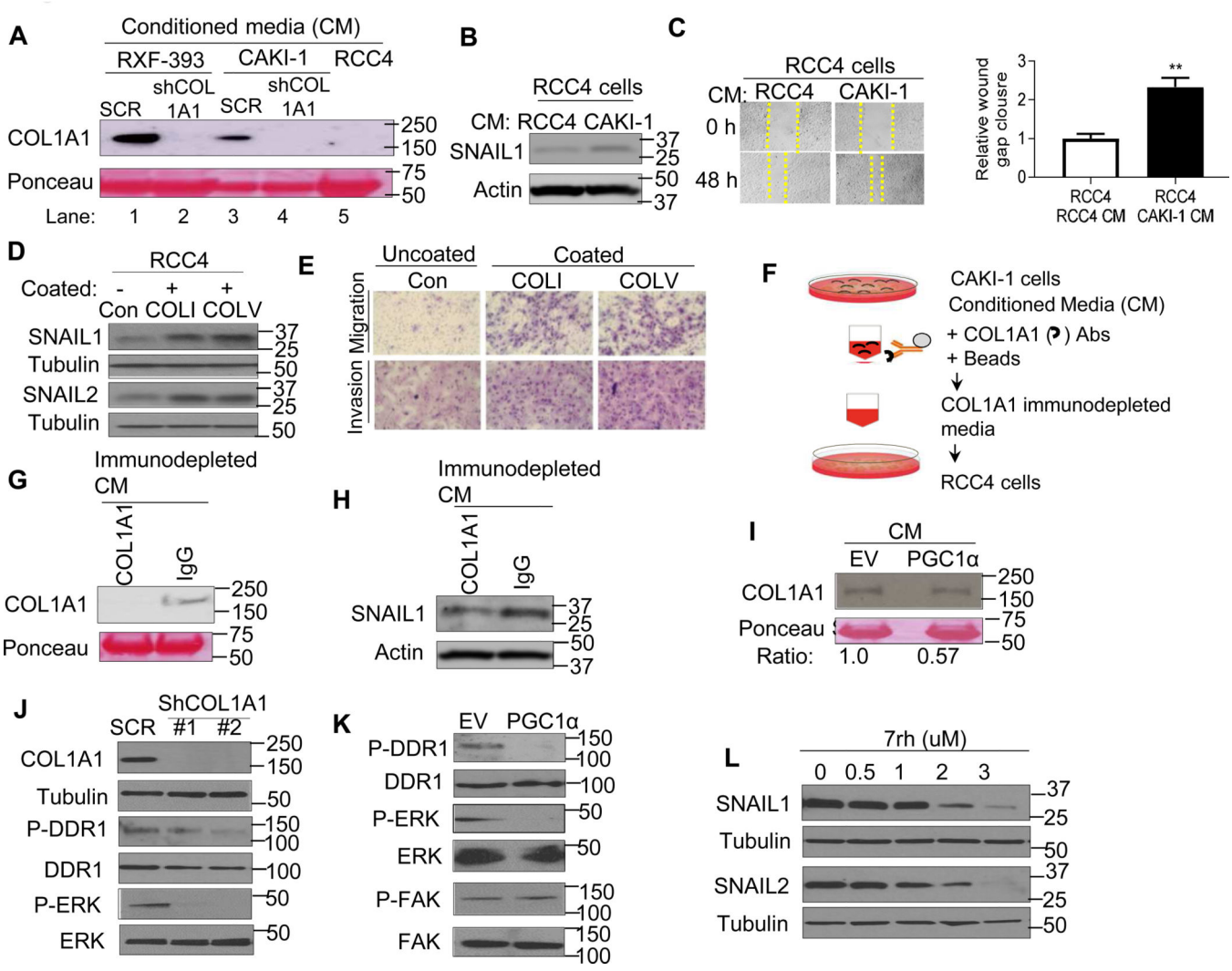

Fig. 6. PGC1α suppresses SNAIL protein via deactivation of collagen-induced DDR1 axis.

(**A**) Western blot analysis of COL1A1 in the conditioned media (CM) from RCC cells stably expressing shRNA control (SCR), COL1A1 shRNA, or RCC4 cells. (**B**) Immunoblot analysis of SNAIL1 expression in RCC4 cells cultured with the CM from RCC4 or CAKI-1 cells. (**C**) Representative images and quantification of migratory phenotype in RCC4 cells cultured with the CM from RCC4 or CAKI-1 cells (n=3/group). (**D**) Western blot analysis of indicated proteins in RCC4 cells cultured on a plate pre-coated with either collagen type I (COLI) or collagen type V (COLV) for 72 h. (**E**) Representative images of migratory and invasive phenotype in RCC4 cells cultured on a plate pre-coated with either collagen type I (COLI) or collagen type V (COLV) for 72 h (n=3/group, 3 independent experiments). (**F**) Illustration of COL1A1 immunodepletion assay. The conditioned media (CM) from CAKI-1 cells were incubated with either COL1A1 antibodies or IgG coated magnetic beads. The COL1A1 immunodepleted media were incubated with RCC4 cells. (**G**) Western blot analysis of COL1A1 in the CM from COL1A1 immunodepletion or IgG control pull down. (**H**) Western blot analysis of SNAIL1 expression in RCC4 cells cultured with the CM from COL1A1 immunodepleted media or IgG control pull down. (**I**) Western blot analysis of

COL1A1 in the CM from CAKI-1 cells stably expressing an EV or PGC1α. (**J**) Western blot analysis of indicated proteins in CAKI-1 cells stably expressing shRNA control (SCR) or two independent shRNA COL1A1. (**K**) Western blot analysis of indicated proteins in CAKI-1 cells stably expressing an EV or PGC1α. (**L**) Immunoblot analysis of indicated proteins in CAKI-1 cells treated with pharmacological DDR1 inhibitor 7rh for 24 h.

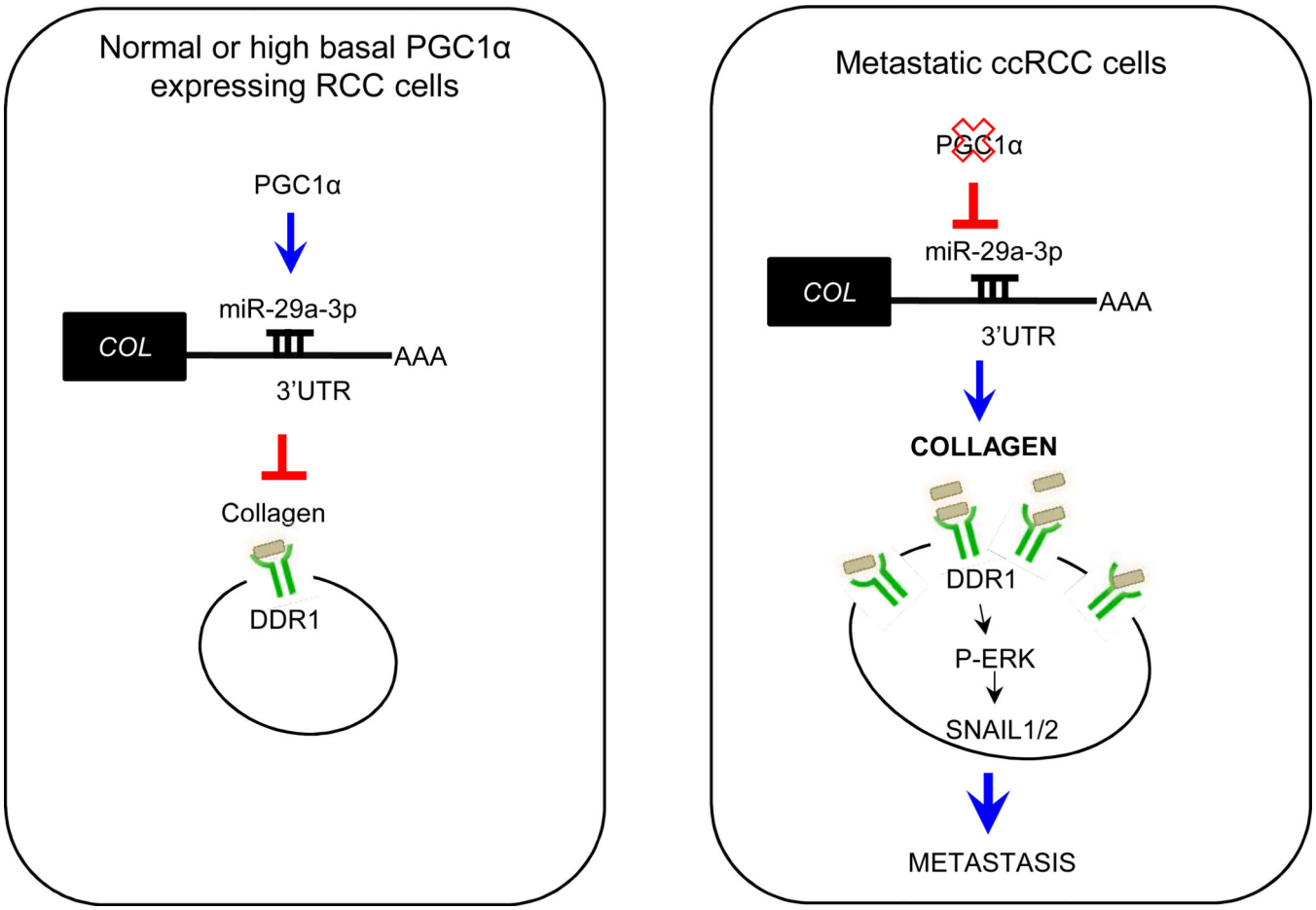

Figure 7. A proposed working model for PGC1α-mediated metastasis suppression.

In normal or high basal PGC1α expressing RCC cells, PGC1α induces *miR-29a* expression which in turn suppresses *COL* mRNA levels. Decreased *COL* expression by the PGC1α / *miR-29a* axis inhibits DDR1/ERK signaling thereby leading to SNAIL degradation. Loss of PGC1α results in stabilization of the prometastatic factors SNAIL1/2.